

Methods, fluxes and sources of gas phase alkyl nitrates in the coastal air

Alin C. Dirtu · Anna J. Buczyńska · Ana F. L. Godoi ·
Rodrigo Favoreto · László Bencs · Sanja S. Potgieter-Vermaak ·
Ricardo H. M. Godoi · René Van Grieken · Luc Van Vaeck

Received: 13 August 2013 / Accepted: 6 June 2014 / Published online: 22 June 2014
© Springer International Publishing Switzerland 2014

Abstract The daily and seasonal atmospheric concentrations, deposition fluxes and emission sources of a few C3–C9 gaseous alkyl nitrates (ANs) at the Belgian coast (De Haan) on the Southern North Sea were determined. An adapted sampler design for low- and high-volume air-sampling, optimized sample extraction and clean-up, as well as identification and quantification of ANs in air samples by means of gas chromatography mass spectrometry, are reported. The total concentrations of ANs ranged from 0.03 to 85 pptv and consisted primarily of the nitro-butane and nitro-pentane isomers. Air mass backward trajectories were calculated by the Hybrid Single-Particle Lagrangian Integrated Trajectory (HYSPPLIT) model to determine the influence of main air masses on AN levels in the air. The

shorter chain ANs have been the most abundant in the Atlantic/Channel/UK air masses, while longer chain ANs prevailed in continental air. The overall mean N fluxes of the ANs were slightly higher for summer than those for winter-spring, although their contributions to the total nitrogen flux were low. High correlations between AN and HNO₂ levels were observed during winter/spring. During summer, the shorter chain ANs correlated well with precipitation. Source apportionment by means of principal component analysis indicated that most of the gas phase ANs could be attributed to traffic/combustion, secondary photochemical formation and biomass burning, although marine sources may also have been present and a contributing factor.

Electronic supplementary material The online version of this article (doi:10.1007/s10661-014-3866-7) contains supplementary material, which is available to authorized users.

A. C. Dirtu · A. J. Buczyńska · R. Favoreto · L. Bencs ·
R. Van Grieken · L. Van Vaeck
Department of Chemistry,
University of Antwerp (UA),
Universiteitsplein 1, 2610 Antwerp, Belgium

A. C. Dirtu
Department of Chemistry,
“Al. I. Cuza” University of Iasi,
700506 Iasi, Romania

A. F. L. Godoi · R. H. M. Godoi
Department of Environmental Engineering,
Federal University of Paraná (UFPR),
Curitiba, Paraná, Brazil

L. Bencs (✉)
Institute for Solid State Physics and Optics, Wigner Research
Centre for Physics, Hungarian Academy of Sciences,
POB 49, 1525 Budapest, Hungary
e-mail: bencs.laszlo@wigner.mta.hu

S. S. Potgieter-Vermaak
Division of Chemistry and Environmental Science,
Manchester Metropolitan University,
Chester Street, Manchester M1 5GD, UK

S. S. Potgieter-Vermaak
Molecular Science Institute, School of Chemistry,
University of the Witwatersrand,
Private Bag X3, PO Wits, Johannesburg 2050, South Africa

Keywords Organic nitrates · N-nutrients · High-volume air sampler · GC-ITMS · Breakthrough volume · Source identification

Introduction

Photochemical processes and oxidant chemistry in the atmosphere are influenced by nitrogen oxides, ozone, hydrocarbons (HCs), and organosulphur compounds (Crutzen 1979; Logan et al. 1981; Liu et al. 1983; Altshuller 1986; Toon et al. 1987). Amongst these, the gaseous alkyl nitrates (ANs or RONO_2) are of particular interest, especially within the ozone/nitrogen oxide system, because their formation and degradation play an important role in tropospheric ozone production (Atkinson et al. 1982; Singh 1987; Luke and Dickerson 1988; Roberts and Fajer 1989; Roberts 1990). The formation of ANs via oxidation of parent hydrocarbons has been a well-known atmospheric mechanism since the 1970s (Darnall et al. 1976). Since the formation of ozone and organic nitrates proceed through the same reaction, monitoring the air concentrations of organic nitrates can provide information on the role of various peroxy radicals in photochemical ozone formation (Flocke et al. 1991). Apart from photochemical formation, ANs could also have an oceanic origin (Walega et al. 1992; Atlas et al. 1993; Chuck et al. 2002; Ballschmiter 2002). Moreover, biomass burning has been observed as a major point source for C_1 – C_4 ANs, although these emissions are not expected to impact global reactive nitrogen levels significantly (Simpson et al. 2002). The primary AN sinks are reported to be photolysis and reactions with hydroxyl radicals (Roberts 1990; Clemitshaw et al. 1997; Talukdar et al. 1997; Russo et al. 2010; Aschmann et al. 2011), although the influence of photochemical AN loss decreases with increasing atomic number (Clemitshaw et al. 1997; Talukdar et al. 1997).

Several studies have been devoted to investigate the temporal (daily, seasonal) variations and geographical distributions of ANs (e.g. Atlas 1988; Simpson et al. 2006). Airborne measurements have shown alkyl and multifunctional nitrates (ΣANs) to be a significant fraction (~10 %) of reactive nitrogen (NO_y) in a number of different chemical regimes (Perring et al. 2010). They have drawn three important conclusions: (1) Correlations of ΣANs with odd oxygen (O_x) indicate a stronger role for ΣANs in the photochemistry of Mexico City

than is expected on the base of current photochemical mechanisms, (2) ΣAN formation suppresses peak O_3 production rates by as much as 40 % near Mexico City and (3) ΣANs play a significant role in the transport of NO_y from Mexico City to the Gulf Region. ANs have also been proven to form in air, where pollution originates from oil spill accidents (Neuman et al. 2012).

The atmospheric nitrogen input, especially at coastal regions, triggers increasing interest in the scientific community. Specifically, atmospheric nitrogen fluxes, in terms of inorganic and organic nitrogen deposition, are important to be assessed to gain insight into their contribution to eutrophication processes at coastal regions.

The low air concentrations of ANs and the complexity of the atmospheric system in terms of organic gas phase and aerosol components with a wide range of polarity make sampling, direct detection and quantification of ANs in the ambient air a challenging task. Sampling of gas phase ANs in air has been performed in several ways, using Tenax adsorption columns (Luxenhofer et al. 1994; Fischer et al. 2000, 2002), a combination of Tenax cartridges and polyurethane (PU) foam (Luxenhofer et al. 1994), silicagel and PU foam (Luxenhofer et al. 1996), silicagel and Tenax (Schneider et al. 1998; Schneider and Ballschmiter 1999) or even charcoal (Atlas and Schauffler 1991; De Kock and Anderson 1994). Simpson et al. (2006) pre-concentrated trace gases from air samples by passing ~1.5 L of canister air through a stainless steel tube filled with 1/8-in diameter glass beads and immersed in liquid nitrogen. A mass flow controller with a maximum allowed flow of 500 mL min^{-1} regulated the trapping process. The trace gases were re-volatilized using a hot water bath and then reproducibly split into five streams for detection.

Generally, organic nitrates have been measured by high-resolution (HR) gas chromatography (GC) with electron capture detection (ECD) (De Kock and Anderson 1994; Moschonas and Glavas 2000; Glavas 2001; Glavas and Moschonas 2001; Fischer et al. 2002; Simpson et al. 2006; Russo et al. 2010; Zhang et al. 2013) and a combination of GC-ECD and GC-MS (Luxenhofer et al. 1994, 1996; Schneider et al. 1998; Schneider and Ballschmiter 1999; Fischer et al. 2000).

Both traditional injections of a concentrated extract (De Kock and Anderson 1994; Luxenhofer et al. 1994, 1996; Schneider et al. 1998; Schneider and Ballschmiter 1999), as well as thermal desorption from adsorption traps and cryo-trapping, have been applied in the

analysis of ANs (Fischer et al. 2000, 2002; Moschonas and Glavas 2000). Nevertheless, pre-separation of ANs is still a critical step of the chemical analysis. For this purpose, diverse procedures have been described, such as adsorption chromatography on silicagel (Luxenhofer et al. 1996; Schneider and Ballschmiter 1999) or normal phase high-performance liquid chromatography with an organonitrate stationary phase (Fischer et al. 2000).

Within the framework of a study aiming at the characterization of nitrogen-containing organic compounds in the marine environment, it appeared to be necessary to develop a sensitive and robust analytical procedure for the determination of ANs. In this paper, an adapted and a further developed design of an air sampler for the low- and high-volume collection of gaseous and aerosol phases of atmospheric ANs are reported. Extraction, clean-up and GC ion trap mass spectrometry (ITMS) identification and quantification have been optimized as well. The preparation of suitable standards of various C3–C9 AN compounds for method calibration is discussed. The daily and seasonal air levels and deposition fluxes of these gas phase ANs together with the identification of possible emission sources of these compounds are also reported.

Experimental

Sampling and weather data collection

A common high-volume (HiVol) sampler has been re-designed for the combined collection of aerosol and gas phase components of the ambient air using either a low- or high-capacity gas adsorption trap (see [Supplementary Information](#)). Daily (24-h) atmospheric air samples were taken 4 days a week (by starting at 14:00 GMT) at a small coastal research/meteorological station of the Flanders Marine Institute (VLIZ), located in De Haan, Belgium (51° 17' 12.77" N, 3° 03' 39.53" E, 6 m a.m.s.l.), during 2 weeks in August 2005 and 5 months (February–April and June–July) in 2006. Wind direction (WD), wind speed (WS), precipitation, relative humidity (RH), air pressure (P_{air}) and air temperature (T_{air}) were monitored and logged by a computer every minute on each day of the sampling campaigns.

For collecting atmospheric PM, a glass fibre filter (Whatmann GF 25) was fitted into the HiVol sampler. Gas phase sampling with low-capacity adsorption traps was achieved using 2 g of 60–80 mesh Tenax-TA®

(Buchem BV, Apeldoorn, the Netherlands) in each of the four tubes of the sampler. The ANs were pre-extracted from the adsorbent with acetone in a Soxhlet-column under reflux for 8 h. A total volume of less than 20 m³ was sampled at a flow rate of 3 m³ h⁻¹ over the four traps. Alternatively, the high-capacity adsorption trap was filled with 100 g of 35–70 mesh, silicagel (Sigma Aldrich NV/SA, Bornem, Belgium) for capturing the gas phase ANs. The silicagel was washed before sampling with a 4:1 (v/v) mixture of pentane-dichloromethane and activated in an electric oven at 160 °C for 24 h. For each sample, an air volume of typically 250 m³ was pumped through at a flow rate of 10 m³ h⁻¹. The chemicals applied in this work were of analytical grade or better, if not stated otherwise. Ultrapure MilliQ water and organic solvents were applied for cleaning, dissolution and dilution (see [Supplementary Information](#)).

Synthesis of alkyl nitrate standards

Apart from the commercially available isopropyl and isobutyl nitrate (99 % purity, Aldrich Chem. Co., Steinheim, Germany), the other studied ANs were synthesized in the UA laboratory to produce high-purity standards for the calibration of the GC-ITMS method. The corresponding alkyl halides (i.e. iodides for methyl and 2-butyl nitrates and corresponding bromide for other ANs synthesized) were dissolved in $\sim 10^{-3}$ mol L⁻¹ acetonitrile, then mixed with a solution of silver nitrate in acetonitrile, containing a two-fold excess of the equivalent amount needed in the reaction, and stirred for 24 h in the dark at room temperature (RT) (Ferris et al. 1953; Luxenhofer et al. 1994). During reaction, ANs segregated as a distinct layer at the top of the aqueous solution and were separated using an extraction funnel. The extract, containing the ANs, was washed with water and dried over Na₂SO₄. Afterwards, the ANs were recovered from the drying agent with dichloromethane. The reaction yields for these syntheses were higher than 95 %. The nomenclature used in this paper for ANs is according to Schneider and Ballschmiter (1996) and Fischer et al. (2002); for instance, 1C3 and 2C5 stand for 1-butyl nitrate and 2-pentyl nitrate, respectively (see Table S1 in [Supplementary Information](#)).

Extraction and clean-up procedures

Subsequent Soxhlet extraction using 150 mL of acetone and pentane (8 h for each), respectively, enabled the

recovery of the gas phase AN compounds from the Tenax TA[®] adsorbents. The excess solvent was evaporated at RT under a gentle nitrogen flow to obtain a sample volume of 0.5 mL. Additional sample clean-up utilized a glass column with an internal diameter (ID) of 10 mm, containing 4 g Florisil (100–200 mesh, Fluka, Buchs, Switzerland), activated before use at 120 °C for 12 h. Pentane was used as an eluent, and the fraction between 9 and 27 mL was kept for analysis. Subsequently, the sample volume was reduced to about 0.5 mL under a nitrogen stream at RT, and the samples were stored at –20 °C in a deep freezer prior to GC-MS injection.

The captured organic compounds, including ANs, were eluted from the silicagel samples with a 400-mL aliquot of 4:1 (v/v) mixture of pentane-dichloromethane in a water-cooled glass column (25.6-cm length, 4-cm ID) (Schneider and Ballschmiter 1999). The extract was concentrated to 150 µL at RT under a gentle nitrogen flow. 2-Fluoro-toluene was used as a recovery standard and an internal standard for the optimization steps and for the GC-MS analysis.

GC-ITMS separation, detection and quantitation

All measurements were performed on a Saturn 2000 GC-ITMS (Varian Inc., Lake Forest, CA, USA). A VF-1 ms capillary column (100 % dimethylpolysiloxane, Varian Inc.; 30 m×0.25 mm ID×1 µm film thickness) was applied with a helium flow rate of 1 cm³ min^{–1}. Sample aliquots of 1 µL were injected using splitless mode. The temperatures of the injector, the transfer line and the ion trap (IT) were set at 250, 220 and 240 °C, respectively. The temperature program for the GC oven was as follows: 40 °C for 5.8 min, increase to 51 °C with 3 °C min^{–1} and hold for 2 min, increase to 75 °C with 3.5 °C min^{–1} and hold for 3.5 min, increase to 96 °C with 5 °C min^{–1} and hold for 2.5 min and increase with 10 °C min^{–1} to 260 °C and hold for 8.13 min. A total chromatographic cycle of 51 min provided the best separation for all AN isomers detected in the air samples. The mass-selective detection, following EI of ANs, was based on the formation of the intense NO₂⁺ fragment at *m/z* 46. Analytical performance data of the developed GC-ITMS method are listed in Table S2. The limits of detection (LODs) obtained with this method (0.001–0.005 pptv) are sufficiently low to quantify the study ANs in most of the samples on the condition that an air volume of 250 m³ is collected.

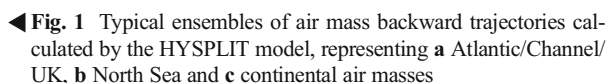
Calculation of air mass trajectories and alkyl nitrate fluxes

Single-tracks and ensembles of air mass backward trajectories (BWTs) were calculated for the start and end time of each day of the sampling by using the Hybrid Single-Particle Lagrangian Integrated Trajectory (HYSPLIT) model (Draxler and Rolph 2003; Rolph 2003). The BWTs were applied to determine the influence of main air masses, i.e. the Atlantic Ocean, the North Sea and the continent, on the air levels of ANs. Typical ensembles of BWTs representing the main air masses are depicted in Fig. 1.

Sea AN fluxes were estimated by using an average literature value (0.027 cm s^{–1}; Hertel et al. 1995), due to the lack of available data for atmospheric dry deposition velocities (*v_d*) of individual ANs over sea surfaces. It has borne in mind that land *v_d* values (both model and experimental) are typically an order of magnitude higher. For example, Hertel et al. (1995) report 0.12 cm s^{–1} for organic nitrates and Russo et al. (2010) 0.13 cm s^{–1} for MeONO₂. This would typically imply a ~4.5 times higher N flux of ANs over land, if the AN air levels and weather conditions are the same. Classification of 24-h N flux data of the individual ANs was based on the origin of the main air masses as determined by the single-track BWTs, i.e. Atlantic/Channel, North Sea, UK, continental or mixed. From these data, the average N fluxes, their fluctuations, expressed as the standard deviation (SD) and the total N contributions were calculated.

Statistical methods

The IBM[®] SPSS[®] Statistics software package (version 20) was used to perform bivariate correlation analysis using two-tailed Pearson's correlation. Since there is no data in the literature on PCA of ANs, their daily concentrations together with the data on inorganic gases and ionic species of PM sampled concurrently (Bencs et al. 2009; Horemans et al. 2009) were processed using PCA, in order to assist the recognition of contributing factors/emission sources. For PCA, Varimax rotation and Kaiser normalization were applied as described in the literature (Costello and Osborne 2005). Principal components (PCs) having eigenvalues higher than 1 in the component data set were retained, i.e. those which could still be classified as plausible emission sources on the basis of the component loadings. In PCs, species having



loadings above 0.7 and below 0.4 were characterized as high and low, respectively. Species having PC loading of less than 0.4 were considered either not be related to the other species or were explored in an additional PC (Costello and Osborne 2005). Reference data on source apportionment published in a comprehensive review (Viana et al. 2008) were also utilized for comparison.

Sampling methodology

The use of adsorption columns is the most common method to collect organic compounds from the gas phase (e.g. Atlas and Schauffler 1991). A critical parameter to be considered is the breakthrough volume of the gas adsorption system. On the one hand, the sampled volume should be as high as possible to facilitate the detection of air components present at ultra-trace levels. On the other hand, overloading of the gas adsorption trap may result in partial losses due to evaporation. It is a common practice to determine the limiting volume by connecting two adsorption columns in series (Atlas and Schauffler 1991; Luxenhofer and Ballschmiter 1994; Schneider and Ballschmiter 1999). However, in this case, the LOD of the analytical method determines the extent, to which the breakthrough volume of the first adsorption column must be exceeded to be able to detect it in the second column.

As an alternative approach, isothermal adsorption chromatography has been applied in the present study. For this purpose, a conventional glass column was packed with an accurately weighed amount of the adsorbent. The retention volume in isothermal elution on a GC-ECD system was determined for at least three temperatures. Plotting the logarithms of the corrected retention volumes as a function of the reciprocal temperature gives a linear relationship, which can be extrapolated with good accuracy to derive a realistic value for the breakthrough volume at the temperature of the air sampling. The breakthrough volumes from 1C3 to 1C7 for 2 g Tenax TA® as adsorbent were 0.5 and 300 m³, respectively. For 1C3 using 100 g silicagel as adsorbent, the value was 310 m³. For this adsorbent, only the breakthrough

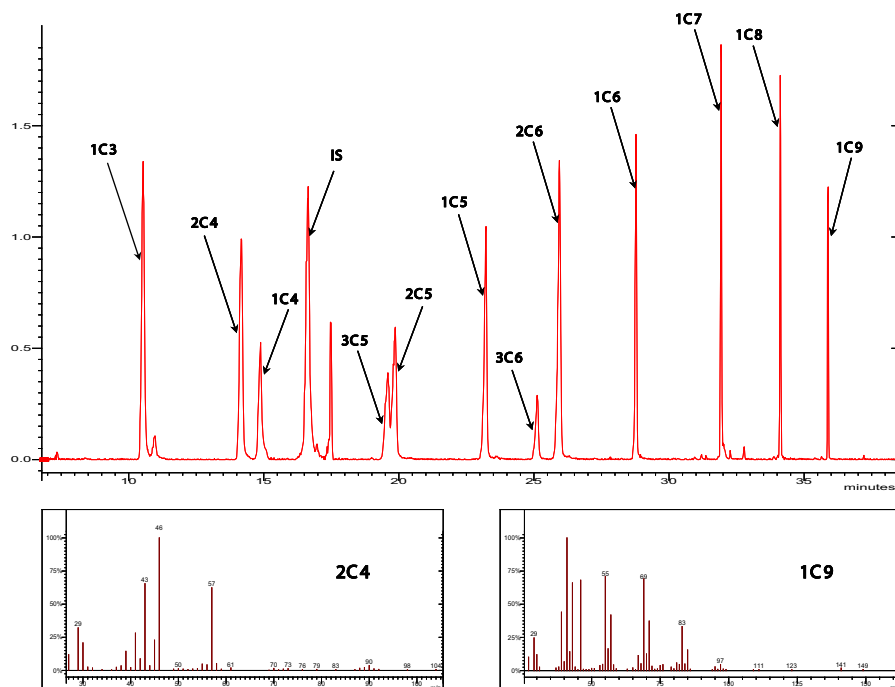


Fig. 2 Mass chromatograms at m/z 46 for a reference mixture of alkyl nitrates (*IS* internal standard) and mass spectra for 2C4 and 1C9

volume for the most volatile AN was determined; otherwise, the retention time would have become too long for AN analogues of longer carbon chains at the maximal allowable column temperature. Specifically, whenever the accurate sampling of C3 is aimed at, the sampling volume should be lower than 0.26 and 3.1 m³ per gram of Tenax TA® and silicagel, respectively. Besides the substantially higher retention capacity of silicagel, it is more cost-effective than Tenax TA®. Thus, it can be advantageously used even in large adsorption traps without any need of adsorbent recovery after extraction and analysis. Therefore, for ambient air sampling, 100 g silicagel was applied in this study. Typical mass chromatograms of the study ANs and mass spectra of 2C4 and 1C9 are depicted in Fig. 2.

Daily and seasonal variations in the air levels of alkyl nitrates

In summer, 11 ANs have been identified and quantified, but only 8 of them were detected in winter-spring (Table 1). The mean air concentrations and the relative abundance of individual AN analogues/isomers have shown seasonal differences. The air levels of individual ANs in the late summer, winter/spring and midsummer seasons ranged from 0.001–0.005 pptv (below LOD) to

78 pptv (Table 1), with median concentrations of 0.07, 0.08 and 0.11 pptv, respectively. These median air concentrations are more representative of a marine/coastal background. These concentrations are generally lower than those reported in the literature for marine air (De Kock and Anderson 1994), although the sampling for the latter was performed at least a decade earlier. The Σ AN fraction investigated consisted primarily of the 1C4, 2C4, 3C5 and 2C5, which is most likely due to the higher photochemical stability of these compounds than those of the higher chain ANs. As known from the literature (Schneider and Ballschmiter 1999), increasing alkyl chain length and photolysis reactions decrease the lifetime of ANs in air. Likewise, the abundances of shorter chain ANs are higher in marine-influenced air masses, which had a higher prevalence than continental air at the site of interest. This could result in higher contributions of the shorter chain AN species to the Σ AN composition.

The daily trends of the Σ AN concentrations and the corresponding (average) weather data are depicted in Fig. 3. High day-to-day variations in the Σ AN levels are observed, with a general decrease in concentrations during periods of high rainfall, RH, temperature and/or wind speed. Literature points out that the efficacy of the atmosphere to act as a sink for ANs increases with enhanced solar radiation, due to increased photolysis

Table 1 Atmospheric alkyl nitrate concentrations and detection frequencies in various seasons over De Haan, Belgium

Parameter	Season	Alkyl nitrate concentration (pptv)												
		1C3	2C4	1C4	3C5	2C5	1C5	3C6	2C6	1C6	1C7	1C8	1C9	ΣAN
Median	Late summer 2005	0.005	0.01	0.006	0.014	0.009	0.005	0.004	0.003	0.005	0.002	0.003	0.002	0.07
	Winter/spring 2006	n.d.	n.d.	0.003	0.048	0.007	0.002	n.d.	0.003	0.003	0.001	0.002	0.002	0.08
	Midsummer 2006	n.d.	n.d.	0.005	0.065	0.008	0.004	n.d.	0.003	0.002	0.001	0.006	0.001	0.11
Range	min	Late summer 2005	n.d.	0.002	0.003	n.d.	0.002	n.d.	n.d.	0.002	n.d.	n.d.	n.d.	~0.04
		Winter/spring 2006	n.d.	n.d.	n.d.	n.d.	n.d.	n.d.	n.d.	n.d.	n.d.	n.d.	n.d.	~0.03
		Midsummer 2006	n.d.	n.d.	n.d.	0.0023	n.d.	n.d.	n.d.	n.d.	n.d.	n.d.	n.d.	~0.03
	max	Late summer 2005	0.008	0.044	0.011	0.073	0.014	0.008	0.007	0.004	0.01	0.004	0.009	0.2
		Winter/spring 2006	n.d.	1.5	0.013	0.54	0.22	0.035	n.d.	0.25	0.38	0.38	0.13	3.5
		Midsummer 2006	n.d.	0.007	6.4	78.8	0.042	0.10	n.d.	0.12	0.22	0.25	0.25	86.4
	1st	Late summer 2005	0.004	0.006	0.004	0.008	0.003	0.004	0.003	0.002	0.004	0.001	0.002	0.04
		Winter/spring 2006	n.d.	n.d.	0.002	0.01	0.004	0.002	n.d.	0.002	0.0013	0.001	0.001	0.03
		Midsummer 2006	n.d.	0.002	0.003	0.037	0.005	0.002	n.d.	0.002	0.0012	0.001	0.002	0.06
Quartiles	3rd	Late summer 2005	0.005	0.026	0.006	0.027	0.012	0.006	0.006	0.004	0.006	0.003	0.005	0.11
		Winter/spring 2006	n.d.	0.0054	0.005	0.16	0.024	0.004	n.d.	0.019	0.014	0.001	0.002	0.25
		Midsummer 2006	n.d.	0.0053	0.006	0.092	0.009	0.01	n.d.	0.006	0.01	0.002	0.04	0.19
Detection frequency (%)	Late summer 2005	13	50	100	50	38	100	38	75	100	88	50	38	n.a.
	Winter/spring 2006	0	2	8	18	11	6	0	16	14	6	3	4	n.a.
	Midsummer 2006	0	0	38	83	7	41	0	41	41	28	55	10	n.a.

ΣAN sum of the study alkyl nitrates (bold), *n.d.* not detected (i.e. below the LOD of the applied method), *n.a.* not applicable

resulting in elevated decomposition rates of ANs (Talukdar et al. 1997).

Furthermore, a seasonal trend is observed, whereby the average winter-spring ΣAN levels are usually higher than during midsummer (Fig. 3). It has to be noted though that occasionally spikes in ΣAN levels in summer have been observed. This is most probably due to the prevailing continental air masses, transporting high pollution loadings to the coastal site. Another factor could be the sporadic higher local traffic density during summer at and around the seaside resort as compared to winter/spring. It is important to note here that these

spikes can mask the regular seasonality of ANs, by producing higher summer ΣAN levels compared to winter/spring. For the above reasons, as a first approach, the spikes for ΣAN levels over 2 pptv were not taken into account in the N flux evaluations as below.

Estimation of alkyl nitrate fluxes

Late summer season in 2005

The highest average daily deposition was observed for 3C5 levels during the prevalence of Atlantic/Channel/

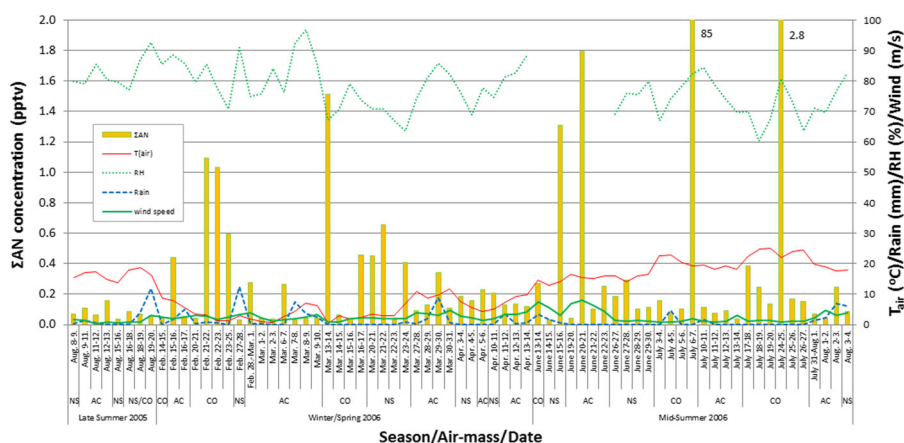


Fig. 3 Daily and seasonal variation of the Σ AN concentration and meteorological parameters (C continental, AC Atlantic/Channel/UK, NS North Sea)

UK air masses ($0.47 \text{ ng N m}^{-2} \text{ day}^{-1}$), followed by lower values for the mixed North Sea/continental air masses ($0.23 \text{ ng N m}^{-2} \text{ day}^{-1}$), but around the LOD values ($0.12 \text{ ng N m}^{-2} \text{ day}^{-1}$) for North Sea air masses. The contribution of 2C4 was also significant when Atlantic/Channel/UK air masses prevailed (i.e. $0.45 \text{ ng N m}^{-2} \text{ day}^{-1}$), whereas lower contributions were found for 1C3, 1C4, 2C5, 1C5, 3C6, 2C6, 1C6 and 1C8 ANs with similar fluxes ($0.02\text{--}0.09 \text{ ng N m}^{-2} \text{ day}^{-1}$). For the North Sea influenced air masses, the contributions from 2C4 and 2C5 were found to be very significant, with average deposition values of 0.14 and $0.12 \text{ ng N m}^{-2} \text{ day}^{-1}$, respectively. Moreover, 1C4, 1C5, 3C6, 2C6 and 1C6 also contributed to the flux, with $0.03\text{--}0.07 \text{ ng N m}^{-2} \text{ day}^{-1}$. Under mixed continental-North Sea influence, the contribution was significant for 1C4, 3C5, 2C5 and 1C9 compounds, with deposition rates of 0.1, 0.23, 0.15 and $0.08 \text{ ng N m}^{-2} \text{ day}^{-1}$, respectively. The 1C5, 3C6, 2C6, 1C6, 1C7 and 1C8 contributed less to the N flux, each with around $0.025\text{--}0.06 \text{ ng N m}^{-2} \text{ day}^{-1}$.

The average fluxes of ANs for the Atlantic/Channel/UK, North Sea and the mixed continental-North Sea air masses were found to be 1.5, 0.72 and $0.96 \text{ ng N m}^{-2} \text{ day}^{-1}$, corresponding to an overall AN flux of $1.1 \text{ ng N m}^{-2} \text{ day}^{-1}$ for this short late summer period. In late summer, the contribution of shorter chain ANs prevails from Atlantic/Channel/UK air masses, while for continental and North Sea air masses, the longer chain ANs also contribute to the N flux of the study ANs (Fig. 4).

Late winter/spring season in 2006

During this period, the average daily flux of 3C5 for all three main air masses was significantly higher than during the late summer period and ranged from 1.1 to $2.5 \text{ ng N m}^{-2} \text{ day}^{-1}$. For the Atlantic/Channel/UK air masses, the average contribution of 3C5 was $1.2 \text{ ng N m}^{-2} \text{ day}^{-1}$, i.e. $\sim 60\%$ of the total flux (Fig. 4). Lower contributions were found for 2C5 and 2C6 (0.26 and $0.12 \text{ ng N m}^{-2} \text{ day}^{-1}$, respectively), whereas the fluxes of 1C4, 1C5, 1C6, 1C8 and 1C9 were much lower, i.e. between 0.05, 0.08, 0.08, 0.03 and $0.03 \text{ ng N m}^{-2} \text{ day}^{-1}$, respectively.

For continental air masses, the distribution of the contribution of the various ANs was more even, with average fluxes of 2.3, 1.1, 0.4, 0.8, 1.4 and $1.1 \text{ ng N m}^{-2} \text{ day}^{-1}$ for 2C4, 3C5, 2C5, 2C6, 1C6 and 1C7, respectively. Negligible contributions for 1C8 and 1C9 with fluxes of 0.07 and $0.03 \text{ ng N m}^{-2} \text{ day}^{-1}$, respectively, have been observed. Similar to the Atlantic/Channel/UK air masses, the 3C5 flux was extremely high ($2.5 \text{ ng N m}^{-2} \text{ day}^{-1}$) and contributed close to 70 % to the total average N flux. The other ANs, characteristic for this air mass, were 2C5, 1C5, 2C6, 1C6 and 1C8 with medium N fluxes, ranging between 0.13 and $0.24 \text{ ng N m}^{-2} \text{ day}^{-1}$. Negligibly, low fluxes for 1C3, 1C4, 2C4, 1C7 and 1C9 were found with values ranging between 0.01 and $0.05 \text{ ng N m}^{-2} \text{ day}^{-1}$.

The average fluxes of ANs for the Atlantic/Channel/UK, continental and North Sea air masses

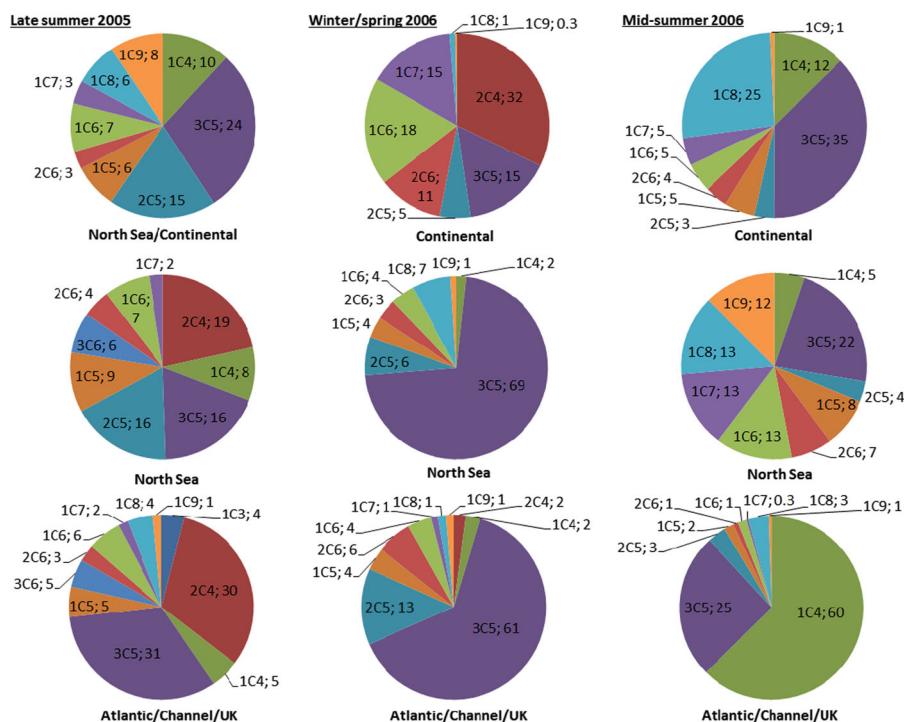


Fig. 4 Percent contributions of individual alkyl nitrates to the N flux of Σ ANs from the main air masses during various seasons

were found to be 2.0, 7.4 and 3.6 $\text{ng N m}^{-2} \text{ day}^{-1}$, corresponding to an overall AN flux of 3.8 $\text{ng N m}^{-2} \text{ day}^{-1}$ for winter/spring. It can be concluded that the highest contribution of AN fluxes originated from air masses approaching from the continent, whereas the contributions of Atlantic and North Sea air masses are 73 and 51 % lower, respectively. The shorter chain ANs were more abundant in marine air masses, while continental air masses were dominated by the longer chain ANs (Fig. 4).

Midsummer season in 2006

Similarly to the late summer period, the Atlantic/Channel/UK air masses are dominated by 3C5, but in this case even more so by 1C4, with average values of 0.9 and 2.1 $\text{ng N m}^{-2} \text{ day}^{-1}$ and total contributions of 25 and 60 %, respectively. The 2C5 and 1C8 compounds also contributed to the N flux, but to a much lower extent than the former ANs, i.e. with depositions around 0.11–0.12 $\text{ng N m}^{-2} \text{ day}^{-1}$. The fluxes of 2C6, 1C5, 1C6 and 1C7 were negligibly small, ranging between 0.01 and 0.06 $\text{ng N m}^{-2} \text{ day}^{-1}$, respectively.

For continental air masses, the daily average 1C4, 3C5 and 1C8 fluxes contributed collectively 72 % to the

total Σ AN budget, with fluxes of 0.26, 0.77 and 0.54 $\text{ng N m}^{-2} \text{ day}^{-1}$, respectively. The fluxes of 1C5, 2C6, 1C6 and 1C7 were lower, ranging between 0.08 and 0.11 $\text{ng N m}^{-2} \text{ day}^{-1}$. During this period, the North Sea air masses showed the more even distribution in contrast to the continental air masses during the late winter/spring period. The most dominant flux was 3C5 with an average value of 0.9 $\text{ng N m}^{-2} \text{ day}^{-1}$. The 1C4, 2C5, 1C5 and 2C6 contributed to the N flux to a varying extent, i.e. 0.21, 0.15, 0.34, 0.28, while the fluxes of 1C6, 1C7, 1C8 and 1C9 were similar, i.e. each $\sim 0.5 \text{ ng N m}^{-2} \text{ day}^{-1}$.

The average fluxes of ANs for the Atlantic/Channel/UK, continental and North Sea air masses were found to be 3.6, 2.2 and 4.1 $\text{ng N m}^{-2} \text{ day}^{-1}$, corresponding to an overall average AN flux of 3.2 $\text{ng N m}^{-2} \text{ day}^{-1}$. Generally, the prevalence of lower chain ANs is observed for Atlantic and continental air masses, while for North Sea air masses, there is a more even distribution between the longer and shorter chain ANs, an observation also made for the late summer period (Fig. 4).

It should be noted that by including the observed spike AN levels (i.e. the values over 2 pptv) into the flux calculations for the midsummer season, the

resultant N flux for continental air masses is $110 \text{ ng N m}^{-2} \text{ day}^{-1}$, which is much higher than the continental N flux observed for winter/spring ($7.4 \text{ ng N m}^{-2} \text{ day}^{-1}$). This corresponds to a reverse seasonal trend than it is expectable on the base of literature (Swanson et al. 2003).

Source apportionment

Correlation analysis

The results for winter-spring and summer show several correlations and seasonal trends between concentrations of ANs and the inorganic species sampled concurrently and the corresponding daily weather data (Table S3). During the winter-spring period, 1C4 is highly correlated with HNO_2 , fine Cl^- , 3C5, 1C5, 2C6, 1C7 and 1C9 air levels but anti-correlated with T_{air} and RH. To some extent, 3C5 showed similar correlations and also correlated with medium- NH_4^+ but anti-correlated with coarse- NH_4^+ and WS. 2C5 correlated to medium and fine $\text{NH}_4^+/\text{NO}_3^-/\text{SO}_4^{2-}/\text{K}^+$ and WS but anti-correlated to T_{air} . 1C5 was also highly correlated with fine Cl^- , 1C4, 3C5, 2C6, 1C7 and 1C9. It is notable that 2C6 and 1C6 are correlated with each other, as well as with HNO_2 and medium- $\text{NH}_4^+/\text{NO}_3^-/\text{SO}_4^{2-}$, which is indicative of their participation in secondary reactions with aerosols, likely via photochemical ways. The resulting HNO_2 may assist in secondary aerosol formation and/or growth. The 2C6 is also related to rain- NO_3^- and P_{air} . The 1C8 was correlated to coarse- NH_4^+ , while 1C9 was anti-correlated to medium- NO_3^- .

In summer, a higher number of between species correlations are experienced compared to the winter-spring season. For instance, 1C4 was strongly correlated with 3C5, 2C6, 1C6, 1C7, 1C9, medium- $\text{NH}_4^+/\text{SO}_4^{2-}/\text{K}^+$ and fine Mg^{2+} . The 3C5 showed the same correlation with the latter inorganic species, but in terms of ANs, it was only correlated with 2C5 and 1C4. 2C5 was correlated with medium/fine $\text{NO}_3^-/\text{SO}_4^{2-}/\text{Na}^+$, fine Cl^- and also with 2C6, 1C6, 1C7 and RH but anti-correlated with 3C5, T_{air} and WS. These results point to a lower extent of 2C5 formation at higher T_{air} (corresponding to higher incoming solar radiation flux) and/or intensified photochemical decomposition of this compound. The 1C5 and 2C6 correlated well with each other

and longer chain ANs. Shorter chain ANs (C3–C5) were generally correlated with medium/fine fractions of $\text{NH}_4^+/\text{SO}_4^{2-}/\text{K}^+$, which points towards sources of biomass burning. The longer chain ANs were related with each other and coarse K^+ . Interestingly, 1C4 and 3C5 correlated well with precipitation in summer.

Principal component analysis

For winter-spring, several PCs have been found (Table S4). PC1 has high loadings for coarse- $\text{Cl}^-/\text{Mg}^{2+}/\text{Ca}^{2+}$ and medium loadings for coarse Na^+ , SO_4^{2-} , NO_3^- , medium-sized Na^+ and Cl^- (representative of sea spray aerosol). Similar loadings have been found for sea salt components sampled over Amsterdam (Vallius et al. 2005), which is also reported to be common for this type of aerosol (Viana et al. 2008). PC2 has high loadings of medium/fine K^+ , fine $\text{NH}_4^+/\text{SO}_4^{2-}$, medium loadings of 2C5 and fine NO_3^- and a low loading for 1C9. Biomass burning has been reported as a source of short chain ANs (Simpson et al. 2002) and also K^+ (Viana et al. 2008). Therefore, it is reasonable to conclude that PC2 accounts for emissions from biomass burning. PC3 has high loadings for coarse $\text{K}^+/\text{NH}_4^+/\text{SO}_4^{2-}$ and medium loadings for coarse $\text{Na}^+/\text{NO}_3^-$ and fine Na^+/Cl^- . This finding is indicative of the formation of coagulated secondary aerosols that are most likely combined with freshly formed sea salt. When including the weather data in the PCA, this component was also closely related to WS and T_{air} , which supports long-range transport. Interestingly, PC4 has high loadings for the longer chain ANs, like 1C6, 2C6 and 1C7, and a low loading for 3C5, while PC6 has high loadings for the shorter chain ANs, i.e. 1C4 and 1C5, a low loading for 2C5 and medium loadings for 3C5 and 1C9. It is presumed that PC4 accounts for the photochemical formation of ANs, most likely through secondary processes in the troposphere, as reported by Atkinson et al. (1982). This is also supported by low loadings of HNO_2 , HNO_3 and medium $\text{NH}_4^+/\text{NO}_3^-/\text{SO}_4^{2-}$. On the other hand, PC6 may suggest a marine source of ANs, which is presumed due to its weak correlation to sea salt components. PC5 has high loadings for medium-sized $\text{NH}_4^+/\text{NO}_3^-/\text{SO}_4^{2-}/\text{Mg}^{2+}$ and medium loadings for HNO_2 and Ca^{2+} , which points towards fossil fuel emissions. PC7 has medium loadings for HNO_3 and medium-size Na^+ , corresponding to local combustion (e.g. cook oven). PC8 has medium loadings for HNO_3 and coarse/medium Ca^{2+} , corresponding to local

background pollution. PC9 has high loadings for NH_3 and medium loadings for HNO_2 . This factor represents emissions originating from extensive animal farming activities from nearby agricultural areas of West Flanders (Bencs et al. 2008).

For the summer season in 2006 (Table S5), PC1 has high loadings for most ANs (i.e. 1C5, 2C5, 1C6, 2C6, 1C7, 1C8 and 1C9) and a medium loading for HNO_3 . These longer chain ANs seem to have the same source in summer, i.e. secondary processes, most likely through photochemical conversion of the corresponding radicals of parent hydrocarbons (Atkinson et al. 1982). PC2 has high loadings for several species of fine PM ($\text{Na}^+/\text{Cl}^-/\text{NO}_3^-/\text{K}^+/\text{Mg}^{2+}/\text{Ca}^{2+}$) and medium loadings for $\text{NH}_4^+/\text{SO}_4^{2-}$, which points towards freshly formed secondary aerosols, possibly through fresh, finely dispersed sea spray particles as nucleation centres (Horemans et al. 2009). PC3 has high loadings for coarse NH_4^+ , Na^+ , K^+ , Mg^{2+} and Ca^{2+} , which points towards soil dust resuspension. PC4 is characterized by high loadings for medium-sized Na^+/Cl^- , which clearly points to sea spray origin, as mentioned above. PC5 is characterized by high loadings for 1C4, 3C5, medium-sized K^+ , medium loadings for medium-sized $\text{NH}_4^+/\text{SO}_4^{2-}$ and low loadings for fine $\text{Mg}^{2+}/\text{SO}_4^{2-}$. This factor most possibly reflects the contribution of biomass burning activities from the nearby agricultural fields. PC6 has a high loading for medium-sized NO_3^- and a medium loading for HNO_2 , medium/fine $\text{NH}_4^+/\text{SO}_4^{2-}$ and coarse NO_3^- , corresponding to secondary aerosol. PC7 has high loadings for coarse $\text{SO}_4^{2-}/\text{Cl}^-$ and a medium loading for NO_3^- , which is indicative of regional/coastal background pollution. PC9 has high loadings for NH_3 and medium loadings for HNO_2 , which represents emissions from animal farming activities as noted above.

Conclusions

The re-designed HiVol sampler allows the simultaneous collection of aerosol and gas phase components of the ambient air using either a low- or high-capacity gas adsorption trap. The adopted sampling protocol and the developed and optimized analytical methodology enabled the accurate determination of gas phase ANs (e.g. those with three to nine carbon atoms) from ambient air samples with minimal pre-separation using the species selectivity and high sensitivity of EI-GC-ITMS.

The N fluxes of the Σ ANs investigated at the coastal sampling site are slightly more pronounced in summer than in winter-spring, although their contribution to the total (wet+dry) nitrogen flux is still considered to be low (cf. Bencs et al. 2009). Higher Σ AN fluxes have been observed from the continent and the North Sea in winter/spring period compared to those from the Atlantic/Channel/UK air masses, in contrast to the summer period during which the fluxes from the latter air mass were also increased. Most of the shorter chain gaseous ANs were correlated with precipitation during the summer period, while during the winter-spring period, the relationship swings more towards the HNO_2 content in air. Some ANs were anti-correlated with air temperature, suggesting a photochemical sink.

Occasional spikes in the AN levels were observed during the summer period, especially if the air over De Haan originated from the continent. These spikes can be attributed to sporadic high local traffic density and more frequent continent air mass dominance during summer compared to winter/spring. It is important to note, however, that these effects can mask the regular seasonality of ANs, reported in the literature, i.e. the peak and the lowest AN air levels in the cold and warm season, respectively (e.g. Swanson et al. 2003).

The PC analysis showed at least three to four sources of gaseous ANs at De Haan (depending on the season), the most important being local combustion (e.g. diesel emissions of vehicular traffic/shipping), secondary photochemical formation from parent hydrocarbons and biomass burning. On the other hand, one cannot rule out the marine origin of a part of the shorter chain ANs (e.g. 1C4, 2C5), they being evidently correlated to certain sea salt aerosol components.

Acknowledgments One of the authors (Alin C. Dirtu) acknowledges an EC grant within Marie Curie program HPMT-CT-2001-00310. The authors are thankful for the technical support provided by Jan Van Loock (UA), André Catrijsse, Frank Broucke and Francisco Hernandez (VLIZ). The authors gratefully acknowledge the NOAA Air Resources Laboratory (ARL) for the provision of the HYSPLIT transport and dispersion model and READY website (<http://www.arl.noaa.gov/ready.html>) used in this publication.

References

- Altshuller, A. P. (1986). The role of nitrogen oxides in nonurban ozone formation in the planetary boundary layer over N.

- America, W. Europe and adjacent areas of ocean. *Atmospheric Environment*, 20(2), 245–268.
- Aschmann, S. M., Tuazon, E. C., Arey, J., & Atkinson, R. (2011). Products of the OH radical-initiated reactions of 2-propyl nitrate, 3-methyl-2-butyl nitrate and 3-methyl-2-pentyl nitrate. *Atmospheric Environment*, 45(9), 1695–1701.
- Atkinson, R., Aschmann, S. M., Carter, W. P. L., Winer, A. M., & Pitts, J. M., Jr. (1982). Alkyl nitrate formation from NO_x-air photooxidations of C₂-C₈ n-alkanes. *Journal of Physical Chemistry*, 86(23), 4563–4569.
- Atlas, E. (1988). Evidence for ≥C₃ alkyl nitrates in rural and remote atmospheres. *Nature*, 331, 426–428.
- Atlas, E., & Schauffler, S. (1991). Analysis of alkyl nitrates and selected halocarbons in the ambient atmosphere using a charcoal preconcentration technique. *Environmental Science & Technology*, 25(1), 61–67.
- Atlas, E., Pollock, W., Greenberg, J., Heidt, L., & Thompson, A. M. (1993). Alkyl nitrates, nonmethane hydrocarbons, and halocarbon gases over the equatorial Pacific Ocean during SAGA 3. *Journal of Geophysical Research*, 98, 16,933–16,949.
- Ballschmiter, K. (2002). A marine source for alkyl nitrates. *Science*, 297(5584), 1127–1128.
- Bencs, L., Ravindra, K., de Hoog, J., Rasoazany, E. O., Deutsch, F., Bleux, N., Berghmans, P., Roekens, E., Krata, A., & Van Grieken, R. (2008). Mass and ionic composition of atmospheric fine particles over Belgium and their relation with gaseous air pollutants. *Journal of Environmental Monitoring*, 10(10), 1148–1157.
- Bencs, L., Krata, A., Horemans, B., Buczyńska, A. J., Dirtu, A. C., Godoi, A. F. L., Godoi, R. H. M., Potgieter-Vermaak, S., & Van Grieken, R. (2009). Atmospheric nitrogen fluxes at the Belgian coast: 2004–2006. *Atmospheric Environment*, 43(24), 3786–3798.
- Chuck, A. L., Turner, S. M., & Liss, P. S. (2002). Direct evidence for a marine source of C₁ and C₂ alkyl nitrates. *Science*, 297(5584), 1151–1154.
- Clemetshaw, K. C., Williams, J., Rattigan, O. V., Shallcross, D. E., Law, K. S., & Cox, R. A. (1997). Gas-phase ultraviolet absorption cross-sections and atmospheric lifetimes of several C₂-C₅ alkyl nitrates. *Journal of Photochemistry and Photobiology A: Chemistry*, 102(2–3), 117–126.
- Costello, A. B., & Osborne, J. W. (2005). Best practices in exploratory factor analysis: four recommendations for getting the most from your analysis. *Practical Assessment Research & Evaluation*, 10(7), 1–9.
- Crutzen, P. J. (1979). The role of NO and NO₂ in the chemistry of the troposphere and stratosphere. *Annual Review of Earth and Planetary Sciences*, 7, 443–472.
- Darnall, K. R., Carter, W. P. L., Winer, A. M., Lloyd, A. C., & Pitts, J. N., Jr. (1976). Importance of RO₂ + NO in alkyl nitrate formation from C₄-C₆ alkane photooxidations under simulated atmospheric conditions. *Journal of Physical Chemistry*, 80(17), 1948–1950.
- De Kock, A. C., & Anderson, C. R. (1994). The measurement of C₃-C₅ alkyl nitrates at a coastal sampling site in the Southern Hemisphere. *Chemosphere*, 29(2), 299–310.
- Draxler, R.R., & Rolph, G.D. (2003). HYSPLIT (HYbrid Single-Particle Lagrangian Integrated Trajectory) Model access via NOAA ARL READY Website (<http://www.arl.noaa.gov/ready/hysplit4.html>). NOAA Air Resources Laboratory, Silver Spring, MD.
- Ferris, A. F., McLean, K. W., Marks, I. G., & Emmons, W. D. (1953). Metathetical reactions of silver salts in solution. III. The synthesis of nitrate esters. *Journal of the American Chemical Society*, 75(16), 4078–4082.
- Fischer, R. G., Kastler, J., & Ballschmiter, K. (2000). Levels and pattern of alkyl nitrates, multifunctional alkyl nitrates and halocarbons in the air over the Atlantic Ocean. *Journal of Geophysical Research, [Atmospheres]*, 105(D11), 14473–14494.
- Fischer, R., Weller, R., Jacobi, H. W., & Ballschmiter, K. (2002). Levels and pattern of volatile organic nitrates and halocarbons in the air at Neumayer Station (70° S), Antarctica. *Chemosphere*, 48(2), 981–992.
- Flocke, F., Volz-Thomas, A., & Kley, D. (1991). Measurements of alkyl nitrates in rural and polluted air masses. *Atmospheric Environment, Part A: General Topics*, 25(9), 1951–1960.
- Glavas, S. (2001). Analysis of C₂-C₄ peroxyacyl nitrates and C₁-C₅ alkyl nitrates with a non-polar capillary column. *Journal of Chromatography A*, 915(1–2), 271–274.
- Glavas, S., & Moschonas, N. (2001). Determination of PAN, PPN, PnBN and selected pentyl nitrates in Athens, Greece. *Atmospheric Environment*, 35(32), 5467–5475.
- Hertel, O., Christensen, J., Runge, E. H., Asman, W. A. H., Berkowicz, R., Hovmand, M. F., & Hov, Ø. (1995). Development and testing of a new variable scale air-pollution model—ACDEP. *Atmospheric Environment*, 29(11), 1267–1290.
- Horemans, B., Krata, A., Buczyńska, A. J., Dirtu, A. C., Van Meel, K., Van Grieken, R., & Bencs, L. (2009). Major ionic species in size-segregated aerosols and associated gaseous pollutants at a coastal site on the Belgian North Sea. *Journal of Environmental Monitoring*, 11(3), 670–677.
- Liu, S. C., McFarland, M., Kley, D., Zafiriou, O., & Huebert, B. (1983). Tropospheric NO_x and O₃ budgets in the equatorial Pacific. *Journal of Geophysical Research: Oceans*, 88(2), 1360–1368.
- Logan, J. A., Prather, M. J., Wofsy, S. C., & McElroy, M. B. (1981). Tropospheric chemistry: a global perspective. *Journal of Geophysical Research: Oceans*, 86(C8), 7210–7254.
- Luke, W. T., & Dickerson, R. R. (1988). Direct measurements of the photolysis rate coefficient of ethyl nitrate. *Geophysical Research Letters*, 15(11), 1181–1184.
- Luxenhofer, O., & Ballschmiter, K. (1994). C₄-C₁₄ alkyl nitrates as organic trace compounds in air. *Fresenius' Journal of Analytical Chemistry*, 350(6), 395–402.
- Luxenhofer, O., Schneider, E., & Ballschmiter, K. (1994). Separation, detection and occurrence of (C₂-C₈)-alkyl- and phenyl-alkyl nitrates as trace compounds in clean and polluted air. *Fresenius' Journal of Analytical Chemistry*, 350(6), 384–394.
- Luxenhofer, O., Schneider, M., Dambach, M., & Ballschmiter, K. (1996). Semivolatile long chain of C₆-C₁₇ alkyl nitrates as trace compounds in air. *Chemosphere*, 33(3), 393–404.
- Moschonas, N., & Glavas, S. (2000). Simple cryoconcentration technique for the determination of peroxyacyl and alkyl nitrates in the atmosphere. *Journal of Chromatography A*, 902(2), 405–411.
- Neuman, J. A., Aikin, K. C., Atlas, E. L., Blake, D. R., Holloway, J. S., Meinardi, S., Nowak, J. B., Parrish, D. D., Peischl, J., Perring, A. E., Pollack, I. B., Roberts, J. M., Ryerson, T. B., & Trainer, M. (2012). Ozone and alkyl nitrate formation from

- the Deepwater Horizon oil spill atmospheric emissions. *Journal of Geophysical Research, [Atmospheres]*, 117(9). Art. D09305.
- Perring, A. E., Bertram, T. H., Farmer, D. K., Wooldridge, P. J., Dibb, J., Blake, N. J., Blake, D. R., Singh, H. B., Fuelberg, H., Diskin, G., Sachse, G., & Cohen, R. C. (2010). The production and persistence of ΣRONO_2 in the Mexico City plume. *Atmospheric Chemistry and Physics*, 10(15), 7215–7229.
- Roberts, J. M. (1990). The atmospheric chemistry of organic nitrates. *Atmospheric Environment, Part A: General Topics*, 24(2), 243–287.
- Roberts, J. M., & Fajer, R. W. (1989). UV absorption cross sections of organic nitrates of potential atmospheric importance and estimation of atmospheric lifetimes. *Environmental Science & Technology*, 23(8), 945–951.
- Rolph, G.D. (2003). Real-time Environmental Applications and Display System (READY) Website. (<http://www.arl.noaa.gov/ready/hysplit4.html>). NOAA Air Resources Laboratory, Silver Spring, MD.
- Russo, R. S., Zhou, Y., Wingenter, O. W., Frinak, E. K., Mao, H., Talbot, R. W., & Sive, B. C. (2010). Temporal variability, sources, and sinks of $\text{C}_1\text{--C}_5$ alkyl nitrates in coastal New England. *Atmospheric Chemistry and Physics*, 10(4), 1865–1883.
- Schneider, M., & Ballschmiter, K. (1996). Separation of diastereomeric and enantiomeric alkyl-nitrates systematic approach to chiral discrimination on cyclodextrin LIPODEX-D. *Chemistry – A European Journal*, 2(5), 539–544.
- Schneider, M., & Ballschmiter, K. (1999). $\text{C}_3\text{--C}_{14}$ -alkyl nitrates in remote South Atlantic air. *Chemosphere*, 38(1), 233–244.
- Schneider, M., Luxenhofer, O., Deissler, A., & Ballschmiter, K. (1998). $\text{C}_1\text{--C}_{15}$ alkyl nitrates, benzyl nitrate and bifunctional nitrates: measurements in California and South Atlantic air and global comparison using C_2Cl_4 and CHBr_3 as marker molecules. *Environmental Science & Technology*, 32(20), 3055–3062.
- Simpson, I. J., Meinardi, S., Blake, D. R., Blake, N. J., Rowland, F. S., Atlas, E., & Flocke, F. (2002). A biomass burning source of $\text{C}_1\text{--C}_4$ alkyl nitrates. *Geophysical Research Letters*, 29(24). Art. 2168, 21/1-21/4.
- Simpson, I. J., Wang, T., Guo, H., Kwok, Y. H., Flocke, F., Atlas, E., Meinardi, S., Rowland, F. S., & Blake, D. R. (2006). Long term atmospheric measurements of $\text{C}_1\text{--C}_5$ alkyl nitrates in the Pearl River Delta region of southeast China. *Atmospheric Environment*, 40(9), 1619–1632.
- Singh, H. B. (1987). Reactive nitrogen in the troposphere. *Environmental Science & Technology*, 21(4), 320–327.
- Swanson, A. L., Blake, N. J., Atlas, E., Flocke, F., Blake, D. R., & Rowland, F. S. (2003). Seasonal variations of $\text{C}_2\text{--C}_4$ nonmethane hydrocarbons and $\text{C}_1\text{--C}_4$ alkyl nitrates at the Summit research station in Greenland. *Journal of Geophysical Research*, 108(D2). Art. 4065, 7/1-7/19.
- Talukdar, R. K., Burkholder, J. B., Hunter, M., Gilles, M. K., Roberts, J. M., & Ravishankara, A. R. (1997). Atmospheric fate of several alkyl nitrates. Part 2. UV absorption cross-sections and photodissociation quantum yields. *Journal of the Chemical Society, Faraday Transactions*, 93(16), 2797–2805.
- Toon, O. B., Kasting, J. F., Turco, R. P., & Liu, S. M. (1987). The sulfur cycle in the marine atmosphere. *Journal of Geophysical Research, [Atmospheres]*, 92(D1), 943–963.
- Vallius, M., Janssen, N. A. H., Heinrich, J., Hoek, G., Ruuskanen, J., Cyrys, J., Van Grieken, R., de Hartog, J. J., Kreyling, W. G., & Pekkanen, J. (2005). Sources and elemental composition of ambient $\text{PM}_{2.5}$ in three European cities. *Science of the Total Environment*, 337(1–3), 147–162.
- Viana, M., Kuhlbusch, T. A. J., Querol, X., Alastuey, A., Harrison, R. M., Hopke, P. K., Winiwarter, W., Vallius, M., Szidat, S., Prévôt, A. S. H., Hueglin, C., Bloemen, H., Wählén, P., Vecchi, R., Miranda, A. I., Kasper-Giebl, A., Maenhaut, W., & Hitzenberg, R. (2008). Source apportionment of particulate matter in Europe: a review of methods and results. *Journal of Aerosol Science*, 39(10), 827–849.
- Walega, J. G., Ridley, B. A., Madronich, S., Grahek, F. E., Shetter, J. D., Sauvain, T. D., Hahn, C. J., Merrill, J. T., Bodhaine, B. A., & Robinson, E. (1992). Observations of peroxyacetyl nitrate, peroxypropionyl nitrate, methyl nitrate and ozone during the Mauna Loa Observatory Photochemistry Experiment. *Journal of Geophysical Research, [Atmospheres]*, 97(D10), 10311–10330.
- Zhang, G., Mu, Y. J., Liu, J. F., & Mellouki, A. (2013). Direct and simultaneous determination of trace-level carbon tetrachloride, peroxyacetyl nitrate, and peroxypropionyl nitrate using gas chromatography-electron capture detection. *Journal of Chromatography A*, 1266, 110–115.